Materials Research. 2021; 24(Suppl 2): e20210317
DOI: https://doi.org/10.1590/1980-5373-mr-2021-0317

Electromechanical Evaluation of Ionomeric Polymer-Metal Composites Using Video Analysis

Matheus Colovati Saccardo[a]*, Ariel Gustavo Zuquello[a], Roger Gonçalves[a], Kaique Afonso Tozzi[a], Rafael Barbosa[a], Laos Alexandre Hirano[b], Carlos Henrique Scuracchio[a]

[a]Universidade Federal de São Carlos, Programa de Pós-Graduação em Ciência e Engenharia de Materiais, Rod. Washington Luiz, Km 235,13565-905, São Carlos, SP, Brasil.
[b]Universidade Federal de Alfenas, Instituto de Ciências e Tecnologia - ICP, Poços de Caldas Alfenas, Minas Gerais, BH, Brasil.

Received: June 28, 2021; Revised: July 19, 2021; Accepted: July 24, 2021

Ionomeric Polymer-Metal Composites (IPMC) are smart materials whose electromechanical behavior depends on the electrical stimulus intensity, membrane hydration level, and ionic migration. This paper investigates the effects of the voltage, relative humidity, and counterion type (Li^+ and K^+) on a Nafion-based IPMC performance. Instrumentation capable of applying an electrical stimulus and measuring the electromechanical response was developed. The ionic conductivity was obtained using Electrochemical Impedance Spectroscopy. Complementary SEM analyses were performed before and after actuation cycles. The IPMC performance improved when the electrical stimulus was 5.00 V, RH = 90%, and Li^+ was used. The IPMC-Li sample is an excellent candidate to be used as an actuator since it exhibited fast actuation movement, considerable displacement, and no evident back-relaxation. However, its mechanical performance decreased over time because of a progressive increase in platinum electrode crack density and dehydration. The video analysis technique is an efficient, effective, and low-cost technique.

Keywords: *IPMC, Smart Materials, Electromechanical Behavior, Displacement, Video Analysis.*

1. Introduction

Ionomeric Polymer Metal Composites (IPMCs) are electroactive materials that can perform bending movements in response to an electrical stimulus and vice-versa. They are based on an ion-exchange polymeric membrane between metallic electrodes[1] and have some interesting properties, such as low density, biocompatibility, and low driven voltage (< 5.00 V)[2,3]. For this reason, they are promising materials for a wide range of applications, such as actuators, sensors, and artificial muscles[4]. Nafion® is the most used polymer to prepare IPMCs due to their high ionic conductivity and chemical, thermal, and structural stability[5]. The ionic conductivity arises from its structure, which has hydrophilic and hydrophobic domains regarding the sulphonated sidechains and polytetrafluorethylene main chain. When the polymer is naturally hydrated, the hydrophilic regions percolate, forming ionomeric microchannels that run through the whole material, where the positively charged counterions responsible for ensuring the electrical neutrality can migrate[6].

To execute the bending movements, electrodes, usually made of noble metals such as gold, platinum, and palladium, are deposited on both sides of the membrane to ensure a homogeneous electric field[7]. The device operation mechanism consists of the hydrated ions that migrate inside ionomeric channels in response to an external electrical field generated between the electrodes. This ionic motion causes a pressure gradient across the membrane, leading to a spatially non-uniform mass accumulation, which causes the device to bend. This electromechanical response depends on the electrical stimulus intensity, counterion type, and membrane hydration level, the last related to environmental conditions, such as relative humidity (RH)[8].

This behavior, related to the interactions between chemical, electrical, and mechanical phenomena, results in non-linear models. Moreover, a back-relaxation phenomenon could be observed when the hydration level is higher than 60%[9]. Since this phenomenon is highly critical for the actuator's performance, several authors have studied this drawback to understand the mechanisms involved in back-relaxation[2,10-14]. Some authors associate this drawback with water counter-diffusion[2]. On the other hand, an effective way to study this phenomenon is through finite element modeling[12,13]. In a recent paper, Leroni and Bardella[11] found that the back-relaxation is intrinsically related to the electrolysis of the water in the vicinity of the electrodes. The water molecule's concentration gradient that forms due to this parallel reaction is the cause of the involuntary reverse movement.

For this reason, modeling, description, and control of IPMC actuators have been a challenge. Accordingly, it is necessary to comprehend the actuator displacement characteristics when operating under different voltages, RH conditions and filled with different counterions. IPMC device electromechanical response is studied in a cantilever

*e-mail: matheusaccardo@hotmail.com

configuration, in which a bar-shaped structural element is anchored at one end while the other remains free to move[15]. The experimental procedure monitors the displacement or the force generated by the device in response to an electrical stimulus as a function of time[16]. Furthermore, IPMCs are usually studied in underwater conditions[17] or with no RH control[18] since no sophisticated experimental apparatus is needed. In this case, a laser or a camera captures the sample free end's movement, measuring its displacement as a function of time[19,20]. A remarkable way to investigate the electromechanical behavior of IPMC samples using video analysis frame by frame was proposed for several papers[21-25].

Tsiakmakis et al.[22] used this technique in comparison with a laser-based measuring instrument. The used visual measurement system was capable of measuring displacements with outstanding performance. However, a complex algorithm and a series of stepwise processes were carried out to obtain the data. Other authors have also used a digital camera monitoring system to evaluate IPMC motion. Bar-Cohen et al.[23] studied IPMC electromechanical performance digitalizing the observed deformation using a CCD camera and an image-processing algorithm. Nemat-Nasser and Wu[24] used a high-speed camera to study the IPMC movement without describing the processing algorithm. The advantages of using a digital camera, aside from the low cost with remarkably monitoring competence, are the non-destructive approach for quantitative deformation and displacement measurement. However, processing algorithms need many computational calculations, making the characterization slow and expensive. In addition, the abovementioned studies did not consider the relative humidity variation effect simultaneously with either laser neither camera systems.

The present study aims to investigate the electromechanical response of Nafion-based IPMC with platinum electrodes (Pt-IPMC) using a digital camera without a processing algorithm and with a highly controllable RH system. The cantilevered IPMC was electrically stimulated while a camera recorded its displacement. A video analysis and modeling tool was used to determine the device's mechanical response (displacement and displacement rate). A square wave signal (1.00 V and 5.00 V amplitude and frequency of 62.50 mHz) was applied on IPMC at RH = 30%, 60%, and 90%. Measurements of electrical current and voltage were carried out using appropriate instrumentation[10]. A water uptake capacity study was performed to determine an empirical relationship between each sample's hydration level as a function of the RH and counterion, and the ionic conductivity was obtained using Electrochemical Impedance Spectroscopy (EIS). Since the actuator's performance over time depends on the integrity of the metallic electrode, the IPMC metallic electrode surface and the electrode/Nafion interface were investigated before and after 225 actuation cycles using Scanning Electron Microscope (SEM). For comparison, two alkaline-metallic cations with different ionic radii that present a linear response were used.

2. Experimental

2.1. Materials and reactants

Nafion®-117 ion-exchange membrane (1100 g mol^{-1} of equivalent weight, acid capacity: 0.89 meq g^{-1} and thickness 177 µm) was purchased from Ion Power. Tetraamineplatinum (II) chloride hydrate [$Pt(NH_3)_4Cl_2$] (98%), sodium borohydride ($NaBH_4$) (90%), and ammonium hydroxide (NH_4OH) (28%) were purchased from Sigma-Aldrich. Lithium chloride (LiCl) and potassium chloride (KCl), both analytical grades from Sigma-Aldrich, were used as received. LiCl and KCl (0.5 mol L^{-1}) solutions were prepared using ultrapure water (Milli-Q method).

2.2. IPMC sample preparation

A modified Oguro's preparation method[8,10,26] was used to assemble the IPMC samples. First, the membrane is immersed in a water solution containing [$Pt(NH_3)_4Cl_2$] and (NH_4OH) for 24 hours. After this period, the membrane is transferred to a beaker with deionized water at 60 °C, and a ($NaBH_4$) solution is added. The Pt ions migrate to the polymer surface and reduce, forming a solid electrode with good electrical conductivity. After sample preparation, the composite was sliced in stripes with 35.00 x 5.00 mm and ion-exchanged with different counterions (Li^+ - 0.69 Å and K^+ - 1.38 Å) through immersing it in a 0.50 mol L^{-1} cation chloride solution for 24 hours.

2.3. Instrumentation

The used instrumentation was based on Hirano's et al.[27] system with some adaptations. It consists of a National Instruments NI-9263 electrical signal generation and a NI-9218 data acquisition platforms, a Texas Instruments (TI) voltage and current amplifier (OPA551), an Arduino-monitored humidity system, an acrylic chamber, and an external digital camera (Sony RX100 IV). Instruments were controlled in real-time by Laboratory Virtual Instrument Engineering Workbench (LabView) software. Figure 1 presents the experimental apparatus used to determine the IPMC electromechanical response and the water uptake capacity.

2.4. Characterization

2.4.1. Water uptake capacity and ionic conductivity

The water uptake capacity is used to determine an empirical relationship between each sample's hydration level as a function of the RH and counterion. Also, this data turns possible to investigate the relationship between the membrane's hydration level and the IPMC electromechanical response. The water uptake capacity was calculated using an RH control system developed to precisely control the relative humidity and measure IPMC mass variations in real-time.

The dried IPMC (80°C for 24 hours) was placed over the load cell inside the acrylic chamber. The chamber was closed, and the humidity control system was activated. With this, the sample starts to absorb water molecules, increasing its mass, quantified in real-time by the NI-9218 data acquisition module. When the mass variation was less than 5%, the sample was assumed to go into osmotic equilibrium (Supplementary material Figure SI.1) with the medium. So, the IPMC water uptake capacity (wt%) as a function of RH could be measured using Equation 1.

$$Water\ Uptake = \frac{W_{wet} - W_{dry}}{W_{dry}} \text{x} 100 \quad (1)$$

Where W(wet) is the mass of the samples after water absorption, and W(dry) is the mass of the wholly dried samples.

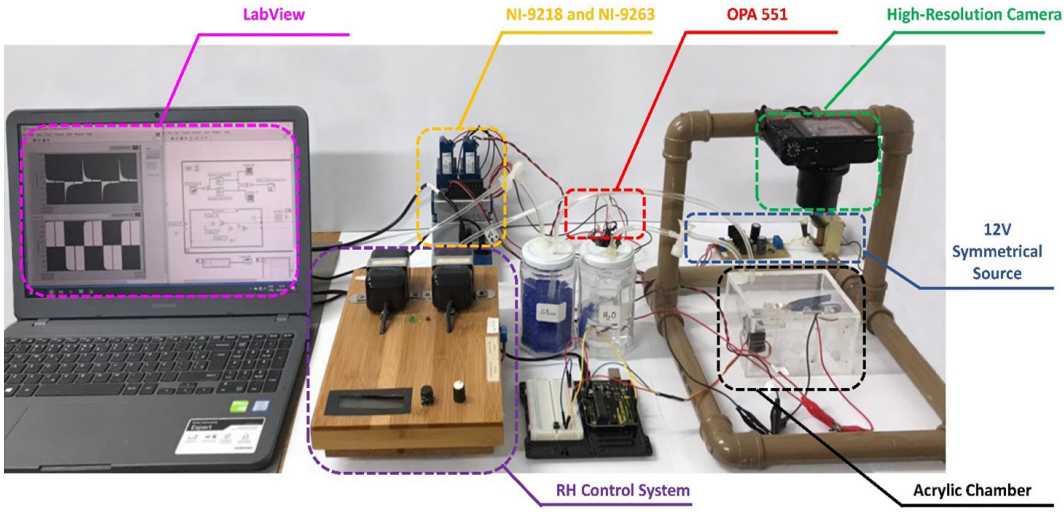

Figure 1. Low-cost system developed for the control and characterization of IPMC devices.

One way to determine the ionic conductivity assumes that the resistance response of the IPMC membrane is a consequence of water and ions present inside the ionomeric channels[28]. Thus, it is possible, through the impedance spectroscopy data, to obtain the ion conductivity (k) can using Equation 2:

$$k = \frac{d}{AR} \tag{2}$$

where R is resistance at low frequency, A is the IPMC area, and d is the thickness of the membrane.

Thus, for this characterization, the ion-exchanged IPMC samples were placed in a faraday cage with controlled humidity and with the aid of the potentiostat/galvanostat/frequency response analyzer Palmsens4 (from PalmSens BV) impedance spectra were collected from 100kHz down to 100mHz with 200 mV of ac perturbation after osmotic equilibrium was reached.

2.4.2. Electromechanical response

Inside the acrylic chamber, the IPMC sample was clamped by copper electrodes in a cantilever configuration. After chamber closing, its humidity was kept for 6 hours to ensure sample osmotic equilibrium with the environment's RH. After this period, a square wave signal was applied (1.00 V and 5.00 V), and the current and voltage responses were acquired using a NI-9263 electrical signal generator module and a NI-9218 data acquisition module. An external digital camera positioned at a distance of 8 cm from the sample was responsible for capturing a video of IPMC actuation. In addition, a free video analysis and modeling software was used to determine the IPMC displacement and displacement rate.

2.4.3. Scanning Electron Microscopy

Additionally, the IPMC metallic electrode surface and the electrode/Nafion interface were investigated before and after 225 actuation cycles using an Inspect™ Scanning Electron Microscope (SEM) model FEI S50 with 25.00 kV and 3000x magnification in SE mode.

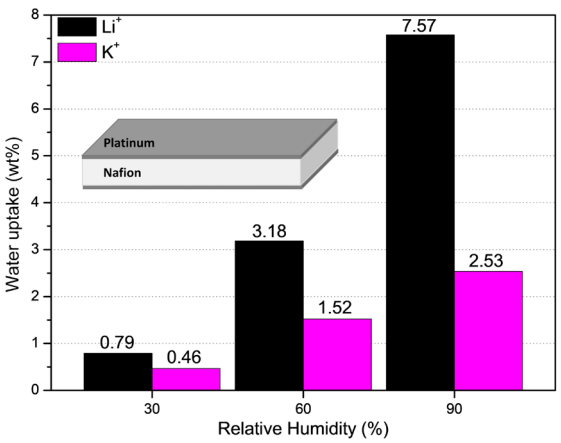

Figure 2. Water uptake capacity as a function of RH (30, 60, and 90%) for IPMC exchanged with Li^+ and K^+ ions. Each sample remained at the desired RH for 6 hours at 25 °C.

3. Results and Discussions

3.1. Water uptake capacity

Figure 2 shows the H_2O absorption capacity as a function of the relative humidity for IPMC samples exchanged with Li^+ and K^+ ions. Each sample remained at the desired RH for 6 hours at 25 °C to ensure that the maximum amount of H_2O molecules was absorbed.

As shown in Figure 2, IPMC samples are highly hygroscopic, and the amount of H_2O molecules absorbed increases as a function of RH and varies according to the counterion size. In general, the water absorption capacity followed the order IPMC-Li > IPMC-K for all tested RH, showing that the smaller the counterion ionic radius, the more water uptake capacity the IPMC will show[10,29,30]. This phenomenon is related to the ionic migration capacity and, consequently, the actuator's electromechanical response, discussed below.

3.2. Electromechanical response

IPMC-Li and IPMC-K electromechanical behavior were studied by applying a square wave (with 1.00 V and 5.00 V) in RH = 30, 60, and 90%. The current and the voltage applied to the sample, the displacement, and the displacement rate response were measured. Figures 3a and 3b present the current and the voltage responses for a 5.00 V bias and RH = 90%. Figures 3c and 3d present the current and the voltage responses for a 1.00 V bias and RH = 30%. For RH = 60% (environment relative humidity), the data obtained are summarized in Table 1.

As observed in Figure 3, the current (A) decreases exponentially over time for each cycle, while the voltage (V) increases exponentially until they reach a quasi-steady state value, which is an RC circuit-like behavior, which is to be expected since the capacitive property is caused by ionic separation occasioned by electrical stimulation. It is also notable that the magnitude of capacitance is related to the diffusion coefficient of the cation present in the IPMC, while the resistance is inversely proportional to it. Furthermore, since the electrical conductivity of the solution inside the Nafion depends on the species present in the ionomeric channels, the resistivity of the IPMC is also affected and, consequently, the resistive-capacitive response of the device. Some authors found that the capacitive properties mainly dominate the electromechanical response of IPMCs[31-33].

Bonomo et al.[34] developed a circuit model to describe the IPMC electrical behavior, explaining that the electric charge accumulation causes the device flexural motions at the anode after an electrical potential is applied. Kocer et al.[32] concludes

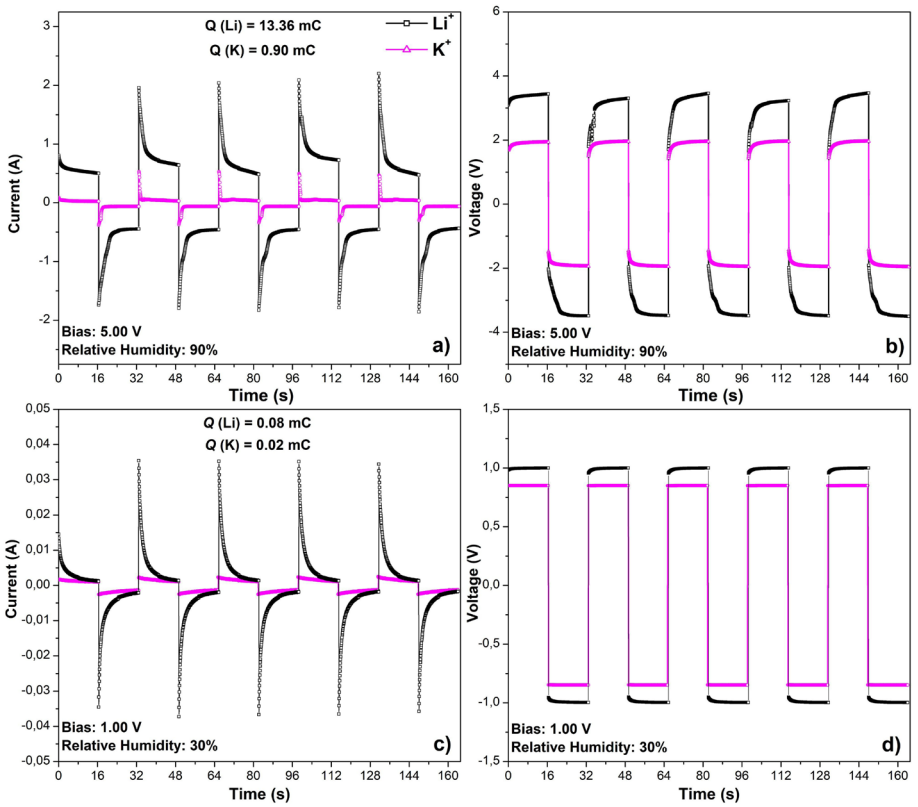

Figure 3. (a) Current and (b) Voltage response for a 5.00 V bias and RH = 90%; (c) Current and (d) voltage for a 1.00 V bias and RH = 30%. IPMC exchanged with Li^+ and K^+. Tests were performed at 25 °C.

Table 1. IPMC displacement and electric charge accumulation data as a function of the applied voltage, RH, water uptake, and counterion.

Voltage (V)	Relative Humidity (%)	Water Uptake (%)		Max. Displacement (mm)		Electrical Charge (mC)	
		IPMC-Li	IPMC-K	IPMC-Li	IPMC-K	IPMC-Li	IPMC-K
1.00 V	30	0.79	0.46	0.40	0.04	0.08	0.02
	60	3.18	1.52	1.62	0.18	0.19	0.05
	90	7.57	2.53	5.45	0.87	0.62	0.11
5.00 V	30	0.79	0.46	9.50	1.15	1.20	0.16
	60	3.18	1.52	16.50	1.75	5.57	0.50
	90	7.57	2.53	27.00	2.72	13.36	0.90

that the primary influence of the capacitive component of IPMC is related to its mechanical response. The stored electrical charge (Q) in the device after voltage application can be calculated by integrating the electric current as a function of time. Numerically, this charge corresponds to the area below the electric current curve as a function of time[34] and could be used to calculate the total device capacitance (Q/V).

As shown in Figure 3, the IPMC-Li and IPMC-K samples presented distinct capacitive behavior when the bias was applied. When RH = 90%, IPMC-Li absorbed three times more water molecules than the IPMC-K. Therefore, its capacitive response was 13 times greater than IPMC-K. On the other hand, when RH = 30%, the water absorption capacity was small for both samples, and, as a consequence, the capacitive response was only four times greater. Hence, the electric charge accumulation inside the membrane is affected by both the membrane hydration level and counterion ionic radius. In other words, IPMC-Li demonstrated a better water uptake capacity and more pronounced capacitive behavior. Furthermore, as Li^+ ions have a smaller ionic radius, they can migrate faster than K^+ ions in experimental conditions.

Consequently, considering several electromechanical models based on ionic migration, the IPMC-Li samples' deformation tends to be more significant. It can be observed in Figure 4, which presents IPMC displacement and displacement rate as a function time. For RH = 60%, the data obtained are summarized in Table 1.

As observed in Figure 4, samples containing distinct counterions behaved differently when the bias was applied, varying the range of motion and profile. Similarly, all sample displacement amplitudes were more visible in a specific direction and decreased over time, indicating a non-uniform mechanical response and a performance loss. As expected, IPMC-Li and IPMC-K showed the maximum displacement observed when the RH = 90% and a 5.00 V bias was applied. Besides, back-relaxation can hardly be observed under cyclic loading since IPMC samples were still moving during the cycle period. When a step voltage is applied, the device bends toward the anode, and, maintaining the voltage constant for a few seconds, the IPMC presents relaxation towards cathode[10].

As stated before, this drawback may occur due to water counter-diffusion (free H_2O molecules migrate towards the opposite direction of solvated cations, causing relaxation)[2] and the asymmetry in the boundary layers of counterion concentration at the membrane-electrode interfaces[11,13]. In this sense, larger cations, low voltages, and short operating times do not present such a phenomenon. For this reason, a minimal movement was observed when the RH = 30%, and a 1.00 V voltage was applied, and no back-relaxation was observed, even after the maximum bending movement. These two mechanisms are present during the operation of these devices. However, they become more evident and pronounced with increasing relative humidity, voltage and decreasing the counterion ionic radius.

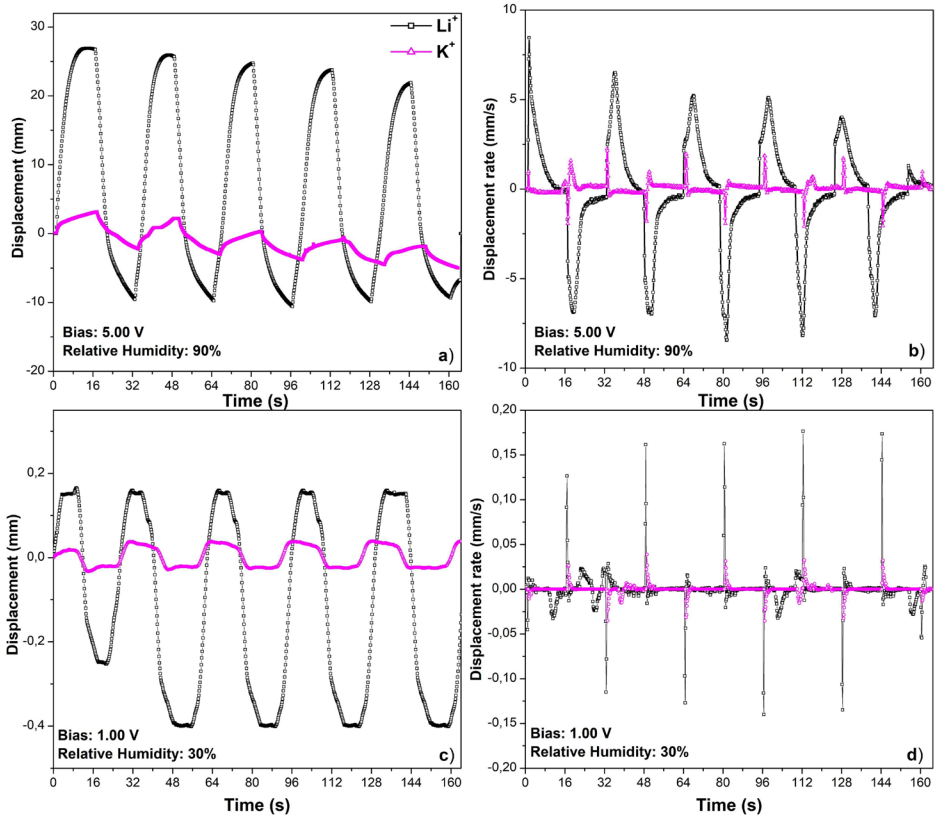

Figure 4. (a) Displacement and (b) Displacement rate response for a 5.00 V bias and RH = 90%; (c) Displacement and (d) Displacement rate response for a 1.00 V bias and RH = 30%. Tests were performed at 25 °C.

Also, IPMC-Li performed a more significant displacement than IPMC-K for all conditions. For example, for the same applied voltage and RH, IPMC-Li has a displacement of at least ten times greater than IPMC-K. This result shows a direct relationship between the water uptake capacity, electric charge accumulation, and electromechanical response. Table 1 summarizes displacement and electric charge accumulation data as a function of the applied voltage, RH, water uptake, and counterion.

After voltage application, solvated ions migrate towards the anode, bringing together water molecules. Once the electrical field is proportional to the voltage, ions are more strongly attracted toward the anode as higher is the potential applied. Furthermore, as the hydration level increases, the amount of the H_2O molecule inside the membrane also increases, and, consequently, the ionomeric channel's width enlarges[6]. Gavach et al.[35] observed that the ionic conductivity as a function of the number of water molecules in these actuators follows the order $H^+ > Li^+ > Na^+ > K^+$. Saccardo et al.[10] showed that water absorption is counterion dependent, and IPMC performance may vary with hydration. Shahinpoor and Kim[36] showed that IPMCs exchanged with Li^+ as counterion presented a displacement of at least 40% higher than IPMCs containing organic counterions. Okada et al.[29] demonstrated that the ion migration increases with the reduction of the counterion size for alkali metals. For this reason, in higher hydration levels, solvated ions can migrate/diffuse quickly, increasing the electrical charge stored at the anode, promoting a more significant displacement.

Figure 5a and 5b shows the Bode plot of the impedance magnitude (|Z|) at each humidity of the IPMC-Li and IPMC-K, respectively. It is possible to observe the differentiated behavior of |Z| depending on the frequency. At low frequencies, it is dominated by the ionic response of the material (slow processes), while, at high frequencies, purely electronic processes are observed, that is, mainly the electrode response. Since the Li^+ solvation layer is much larger than that of K^+ and consequently absorbs more humidity, there is a more significant impact on the low-frequency response with the RH variation and lower |Z| values. In turn, Figure 5c shows the IPMC ionic conductivity variation for RH = 30, 60, and 90% obtained from the impedance data. IPMC-Li shows a more significant variation in conductivity due to the high hygroscopicity of the membrane in the presence of this ion. In addition, once K^+ is a larger and slower ion, it leads the Nafion to present lower ionic conductivity.

Also, this effect causes a variation in the sample displacement rate. Figures 4b and 4d illustrate a displacement rate profile as a function of time for 1.00 V and 5.00 V bias, respectively. As expected, once the voltage was applied, the IPMC sample displacement rate increased over time until it reached the maximum value after a few seconds. After that, this rate decreased until reaching minimum values, showing a clear relationship with the maximum and the minimum value of the electric current passing through the sample. Also, IPMC-Li and IPMC-K presented fast responses in RH = 90% and 5.00 V and slow responses in RH = 30% and 1.00 V. Likewise, for all voltage and RH conditions, IPMC-Li performed a faster displacement than IPMC-K. Therefore, it is evident that the higher voltage, the higher the hydration level of the polymeric membrane, and the smaller counterion promote more significant ionic migration, higher charge accumulation, and more significant and faster displacement.

Finally, it is worth highlighting the camera's monitoring capacity. In general, the technique showed excellent performance and competence to characterize these materials. Also, it is an efficient, effective, and low-cost technique. For example, in Nemat-Nasser and Wu[24], the authors studied with precision the IPMC's high-frequency motion with a high-speed camera (120 frames/sec). On the other hand, Tsiakimakis and Laopoulos[37] used a CCD camera (30 frames/sec) to monitor the IPMC movement underwater (low-frequency condition – 0.5 Hz or less). In both cases, no monitoring problems were observed.

Nevertheless, the author affirms that monitoring problems may appear when high-frequency movements are tracked by limited frame rate cameras (25-30 frames/sec). However, as noted in this paper, the fast bending movement was accurately monitored, and system perturbations were not

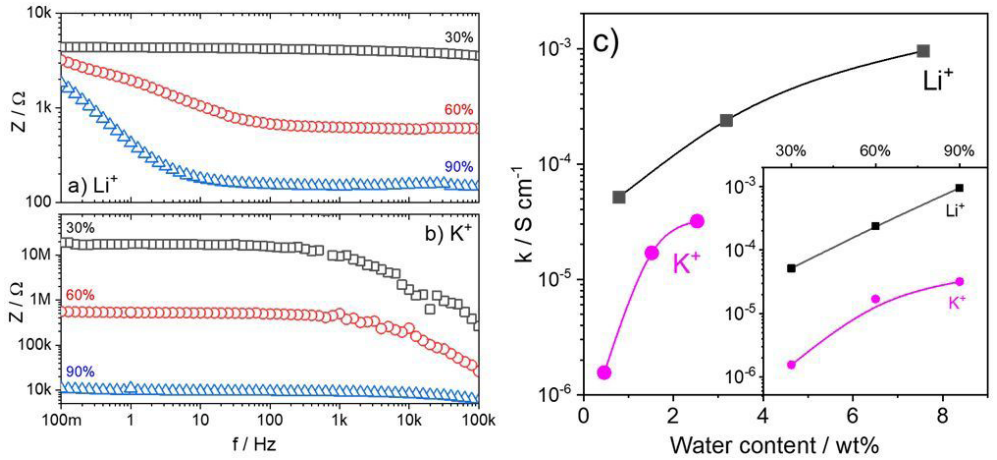

Figure 5. Bode |Z| plots for a) IPMC-Li and b) IPMC-K in several RH conditions and c) ionic conductivity (k) as a function of the IPMC water content (k versus RH inset).

observed. For these reasons, it could be an alternative for IPMC actuator feedback control since it can track position with high speed and precision[38].

3.3. Scanning electron microscopy

The IPMC metallic electrode surface and the electrode/Nafion interface were investigated before and after 225 actuation cycles to verify the platinum surface integrity before and after actuation (Figure 6). Figures 6a and 6d show the IPMC Pt electrode shortly after the IPMC was obtained by the process described in item 2.1. Figures 6b, 6c, 6e, and 6f present SEM images of IPMC-Li and IPMC-K after two hours of uninterrupted actuation (225 cycles). Tests were performed with 5.00 V bias and RH = 90%.

In Figure 6, it is possible to observe the polymer morphology and the Pt layer thickness. The IPMC thickness at RH = 50% (experimental condition) is 195 µm, of which 177 µm corresponds to Nafion-117 and 18 µm to platinum electrode. However, depending on the counterion and environment relative humidity, the device thickness may vary slightly[39]. In addition, the Nafion layer has a stratified morphology, typical of extruded multiphase polymer films. Finally, the polymer/metal interface region showed no imperfections or damage before and after 225 cycles. Therefore, it is possible to affirm that the adhesion between the materials in this region is adequate and did not influence the IPMC performance.

Figure 6d shows that the Pt layer is not homogeneous, and fractures are visible, indicating that cracks are present, even before actuation cycles. These "mud-like" structures are well known and represent the cracks formed during the drying process after the reduction method when the strain caused by the Nafion shrinking exceeds the platinum film's tensile strength[40,41]. After 225 actuation cycles, many micro-fractures in the deposited platinum outcome from the sample's bending motion, increasing crack density in both samples (Figures 6e and 6f). It has been shown that cracks in the electrode surface reduce the platinum layer conductivity, impairing the actuator performance[42]. This drawback is intensified by increasing the displacement amplitude and the number of cycles[43]. Also, under continuous bending cycles, cracks are generated along with the interface of the "mud-like" structure, decreasing the electrode conductivity[44].

As expected, the IPMC-Li sample presented more cracks on the platinum electrode's surface (Figure 6e) since the displacement amplitude was much greater than the IPMC-K sample (Figure 6f). As the device operates over time, the number of cracks increased, reducing the metallic electrode's electrical conductivity. In addition, as the electrical resistance of the electrodes increases, the electric field generated between them decreases. Besides, water evaporation through the cracks and electrolysis[45] may occur, reducing the membrane's water content. Therefore, the ionic migration is reduced, harming the bending movement. Consequently, the IPMC-Li mechanical performance decreased over time, as observed in Figure 7a.

As can be seen, there was a 15% reduction in the performance of the IPMC-Li device. On the other hand, as observed in Figure 7b, the IPMC-K displacement amplitude remained constant even after 225 cycles. Despite the presence of cracks, its performance has not changed over time. In this case, the electrical field generated between the electrodes may overcome the crack effect, maintaining the mechanical response after 225 cycles identical to the initial response. Still, the IPMC-Li displacement is five times greater than that of IPMC-K. The samples would have the same mechanical response only if the IPMC-Li experiences

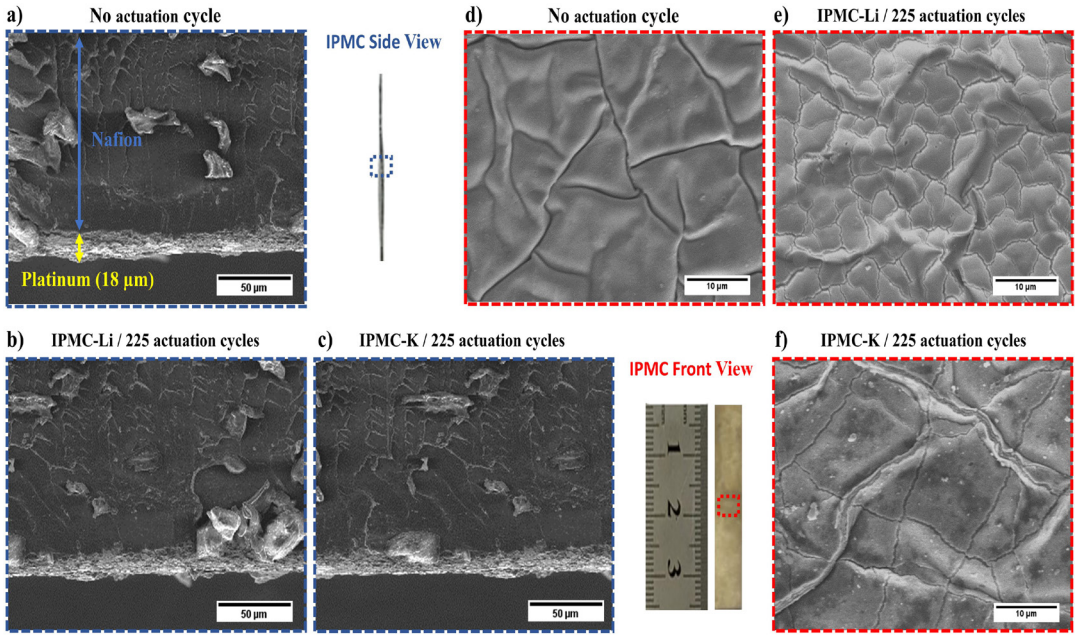

Figure 6. SEM images of IPMC samples; (a) IPMC side view before actuation; (b) IPMC-Li side view after 225 actuation cycles; (c) IPMC-K side view after 225 actuation cycles; (d) IPMC front view before actuation; (e) IPMC-Li front view after 225 actuation cycles; (f) IPMC-K front view after 225 actuation cycles. Tests were performed for 5.00 V bias and RH = 90% at 25 °C.

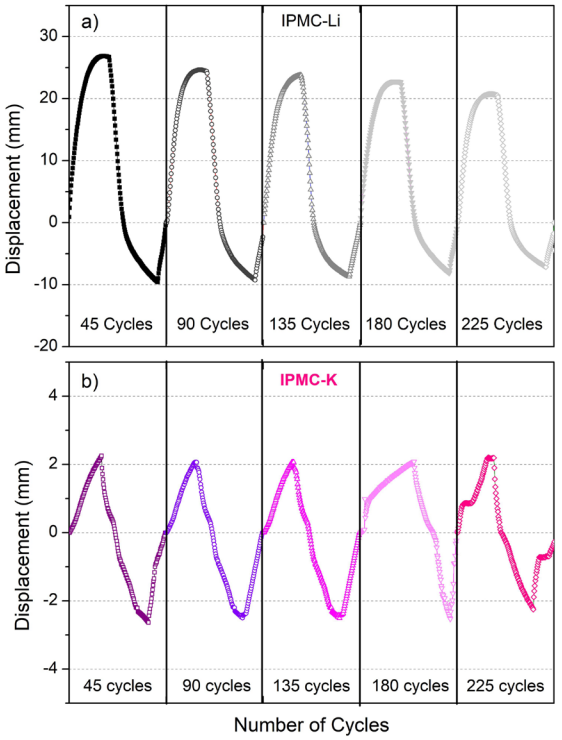

Figure 7. IPMC displacement as a function of the number of cycles. a) IPMC-Li performance; b) IPMC-K performance. Tests were performed for 5.00 V bias and RH = 90% at 25 °C.

an 86% performance reduction. Considering these aspects, the IPMC-Li sample is an excellent candidate to be used as an actuator since it exhibited fast actuation movement, considerable displacement, and no evident back-relaxation under cycling load.

4. Conclusions

Nafion/Pt-based ionic polymer-metal composites exchanged with Li^+ and K^+ counterions had their electromechanical properties investigated using a digital camera without a processing algorithm. Measurements were held controlling the relative humidity (RH = 30%, 60%, and 90%). A water uptake capacity study was performed to determine an empirical relationship between each sample's hydration level as a function of the RH and counterion. The IPMC metallic electrode surface and the platinum/Nafion interface were investigated before and after 225 actuation cycles using Scanning Electron Microscope (SEM).

In general, IPMC samples are highly hygroscopic, and the amount of H_2O molecules absorbed increases as a function of RH and the counterion size. Due to Nafion's water absorption capacity, it is noticeable that ion migration is more significant under higher RH conditions, and electrical charge storage is more pronounced, promoting more significant displacement. The IPMC-Li sample presented a more significant variation in conductivity due to the high hygroscopicity of the membrane in the presence of this ion. On the other hand, the IPMC-K presented a lower ionic conductivity since K^+ is a larger and slower ion. Also, the considerable influence of counterion size was observed since, for the same voltage and RH conditions, the IPMC-Li sample performed a displacement ten times greater than IPMC-K. Similarly, it was observed that the displacement becomes larger and faster with the increase of the applied voltage.

The images obtained by SEM illustrate the morphology of the IPMC Pt electrode, showing that cracks are present before actuation and cracks density increases over time, decreasing mechanical performance. The polymer/metal interface region showed no imperfections or damage before and after 225 cycles, indicating that the bending movement did not influence the adhesion between the platinum and Nafion.

Finally, the camera's monitoring capacity proved to be an excellent alternative to characterize these materials since the technique showed excellent performance and competence to monitor the actuator displacement as a function of time. Also, it is an efficient, effective, and low-cost technique. For these reasons, it could be an alternative for IPMC actuator feedback control since it can track position with high speed and precision. This approach will be investigated in a future paper.

5. Acknowledgements

This study was financed in part by the Coordenação de Aperfeiçoamento de Pessoal de Nível Superior (CAPES) - Finance Code 001. To CAPES for the scholarships process #88887.501393/2020-00, CAPES/DINTER - process #23038.021524/2016-88, CAPES/PROEX - process #88887.335799/2019-00, and CAPES/PRINT - process #88887.569936/2020-00.

The authors would also like to thank the Fundação de Amparo à Pesquisa do Estado de São Paulo (FAPESP) - process #2018/07001-6, #2018/10843-9, #2018/09761-8, and #2020/02696-6. We are also grateful for the support of Conselho Nacional de Desenvolvimento Científico e Tecnológico (CNPq).

6. References

1. Bahramzadeh Y, Shahinpoor M. A review of ionic polymeric soft actuators and sensors. Soft Robot. 2014;1(1):38-52.
2. Shahinpoor M. Ionic Polymer Metal Composites (IMPCs): smart multi-functional materials and artificial muscles. London: Royal Society of Chemistry; 2016. p. 1-60. Fundamentals of Ionic Polymer Metal Composites (IPMCs): RSC Smart Materials.
3. Dong Y, Yeung K-W, Tang C-Y, Law W-C, Tsui GC-P, Xie X. Development of ionic liquid-based electroactive polymer composites using nanotechnology. Nanotechnol Rev. 2021;10(1):99-116.
4. Kim KJ, Palmre V, Stalbaum T, Hwang T, Shen Q, Trabia S. Promising developments in marine applications with artificial muscles: electrodeless artificial cilia microfibers. Mar Technol Soc J. 2016;50(5):24-34.
5. Bar-Cohen Y, Leary SP, Yavrouian A, Oguro K, Tadokoro S, Harrison JS, et al. Challenges to the application of IPMC as actuators of planetary mechanisms. In: SPIE 3987, Smart Structures and Materials 2000: Electroactive Polymer Actuators and Devices (EAPAD); 2000; USA. Proceedings. USA: SPIE; 2000, p. 140.
6. Mauritz KA, Moore RB. State of understanding of nafion. Chem Rev. 2004;104(10):4535-85.
7. Bar-Cohen Y, editor. Electroactive Polymer (EAP) actuators as artificial muscles: reality, potential, and challenges. USA: SPIE; 2004.
8. Gonçalves R, Tozzi KA, Saccardo MC, Zuquello AG, Scuracchio CH. Nafion-based ionomeric polymer/metal composites

operating in the air: theoretical and electrochemical analysis. J Solid State Electrochem. 2020;24(8):1845-56.
9. Vunder V. Modeling and characterization of back-relaxation of ionic electroactive polymer actuators. [thesis]. Tartu: University of Tartu; 2016.
10. Saccardo MC, Zuquello AG, Tozzi KA, Gonçalves R, Hirano LA, Scuracchio CH. Counter-ion and humidity effects on electromechanical properties of Nafion®/Pt composites. Mater Chem Phys. 2020;244:122674.
11. Leronni A, Bardella L. Modeling actuation and sensing in ionic polymer metal composites by electrochemo-poromechanics. J Mech Phys Solids. 2021;148:104292.
12. Porfiri M, Leronni A, Bardella L. An alternative explanation of back-relaxation in ionic polymer metal composites. Extreme Mech Lett. 2017;13:78-83.
13. Porfiri M, Sharghi H, Zhang P. Modeling back-relaxation in ionic polymer metal composites: the role of steric effects and composite layers. J Appl Phys. 2018;123(1):014901.
14. Annabestani M, Sayad MH, Esmaeili-Dokht P, Gorji R, Fard M. Eliminating back relaxation in large-deformable IPMC artificial muscles: a noise-assistive pattern-free electrode approach. In: Proceedings of the 27th National and 5th International Iranian Conference on Biomedical Engineering (ICBME), 2020 Nov 5-60; Tehran, Iran. USA: IEEE; 2020. p. 1-5.
15. Vokoun D, He Q, Heller L, Yu M, Dai Z. Modeling of IPMC Cantilever's Displacements and Blocking Forces. J Bionics Eng. 2015;12(1):142-51.
16. Yang L, Zhang D, Zhang X, Tian A, Wang X. Models of displacement and blocking force of ionic-polymer metal composites based on actuation mechanism. Appl Phys, A Mater Sci Process. 2020;126(5):365-72.
17. Minaian N, Olsen ZJ, Kim KJ. Ionic Polymer-Metal Composite (IPMC) artificial muscles in underwater environments: review of actuation, sensing, controls, and applications to soft robotics. In: Paley DA, Wereley NM, editors. Bioinspired sensing, actuation, and control in underwater soft robotic systems. USA: Springer International Publishing; 2021. p. 117-39.
18. Zhang X, Wang M, Li M, Zhang M, Zhang C. Fabrication of macroporous nafion membrane from silica crystal for ionic polymer-metal composite actuator. Processes (Basel). 2020;8(11):1389-96.
19. Wang HS, Cho J, Park HW, Jho JY, Park JH. Ionic polymer–metal composite actuators driven by methylammonium formate for high-voltage and long-term operation. J Ind Eng Chem. 2021;96:194-201.
20. Guo D, Wang L, Wang X, Xiao Y, Wang C, Chen L, et al. PEDOT coating enhanced electromechanical performances and prolonged stable working time of IPMC actuator. Sens Actuators B Chem. 2020;305:127488.
21. Feng GH, Huang WL. Investigation on the mechanical and electrical behavior of a tuning fork-shaped ionic polymer metal composite actuator with a continuous water supply mechanism. Sensors (Basel). 2016;16(4):1-18.
22. Tsiakmakis K, Brufau-Penella J, Puig-Vidal M, Laopoulos T. A camera based method for the measurement of motion parameters of IPMC actuators. IEEE Trans Instrum Meas. 2009;58(8):2626-33.
23. Bar-Cohen Y, Sherrit S, Lih S-S. Characterization of the electromechanical properties of EAP materials. In: SPIE 4329, Smart Structures and Materials 2001: Electroactive Polymer Actuators and Devices SPIE; 2001; USA. Proceedings. USA: SPIE; 2001. p. 319-60.
24. Nemat-Nasser S, Wu Y. Comparative experimental study of ionic polymer-metal composites with different backbone ionomers and in various cation forms. J Appl Phys. 2003;93(9):5255-69.
25. Li S, Yip J. Characterization and actuation of ionic polymer metal composites with various thicknesses and lengths. Polymers (Basel). 2019;11(1):91-105.
26. Oguro K, Takenaka H, Kawami Y. Actuator element. United States patent *US 5,268,082*. 1993.
27. Hirano LA, Acerbi LW, Kikuchi K, Tsuchitani S, Scuracchio CH. Study of the influence of the hydration level on the electromechanical behavior of nafion based ionomeric polymer-metal composites actuators. Mater Res. 2015;18(suppl 2):154-8.
28. Slade S, Campbell SA, Ralph TR, Walsh FC. Ionic conductivity of an extruded nafion 1100 EW series of membranes. J Electrochem Soc. 2002;149(12):A1556.
29. Okada T, Xie G, Gorseth O, Kjelstrup S, Nakamura N, Arimura T. Ion and water transport characteristics of Nafion membranes as electrolytes. Electrochim Acta. 1998;43(24):3741-7.
30. Nemat-Nasser S. Micromechanics of actuation of ionic polymer-metal composites. J Appl Phys. 2002;92(5):2899-915.
31. Akle BJ, Leo DJ, Hickner MA, McGrath JE. Correlation of capacitance and actuation in ionomeric polymer transducers. J Mater Sci. 2005;40(14):3715-24.
32. Kocer B, Zangrilli U, Akle B, Weiland L. Experimental and theoretical investigation of ionic polymer transducers in shear sensing. J Intell Mater Syst Struct. 2015;26(15):2042-54.
33. Lumia R, Shahinpoor M. IPMC microgripper research and development. J Phys Conf Ser. 2008;127:012002.
34. Bonomo C, Fortuna L, Giannone P, Graziani S, Strazzeri S. A resonant force sensor based on ionic polymer metal composites. Smart Mater Struct. 2008;17(1):015014.
35. Gavach C, Pamboutzoglou G, Nedyalkov M, Pourcelly G. AC impedance investigation of the kinetics of ion transport in Nafion® perfluorosulfonic membranes. J Membr Sci. 1989;45(1-2):37-53.
36. Shahinpoor M, Kim KJ. Effects of counterions on the performance of IPMCs. In: Smart Structures and Materials 2000: Electroactive Polymer Actuators and Devices (EAPAD); 2000; USA. Proceedings. USA: SPIE; 2000. p. 110-22.
37. Tsiakmakis K, Laopoulos T. An improved tracking technique for visual measurements of ionic polymer–metal composites (IPMC) actuators using Compute Unified Device Architecture (CUDA). Meas Sci Technol. 2011;22(11):114006.
38. Kamamichi N, Takagi K, Sano S. Modeling and feedback control of electro-active polymer actuators. In: Asaka K, Okuzaki H, editors. Soft actuators. USA: Springer; 2014. p. 327-41.
39. Bendert JC, Papadias DD, Myers DJ. The effect of Na+ impurities on the conductivity and water uptake of nafion 115 polymer electrolyte fuel cell membranes. J Electrochem Soc. 2010;157(10):1486-90.
40. He Q, Yu M, Yang X, Kim KJ, Dai Z. An ionic electroactive actuator made with graphene film electrode, chitosan and ionic liquid. Smart Mater Struct. 2015;24(6):065026.
41. Lu J, Kim S-G, Lee S, Oh I-K. A biomimetic actuator based on an ionic networking membrane of poly(styrene- alt -maleimide)-incorporated poly(vinylidene fluoride). Adv Funct Mater. 2008;18(8):1290-8.
42. Stoimenov BL, Rossiter JM, Mukai T. Anisotropic surface roughness enhances the bending response of ionic polymer-metal composite (IPMC) artificial muscles. In: SPIE 6413, Smart Materials IV; 2006; USA. Proceedings. USA: SPIE; 2006. p. 641302.
43. Lee S-G, Park H-C, Pandita SD, Yoo Y. Performance improvement of IPMC (Ionic Polymer Metal Composites) for a flapping actuator. Int J Control Autom Syst. 2006;4:748-55.
44. Park K, Yoon MK, Lee S, Choi J, Thubrikar M. Effects of electrode degradation and solvent evaporation on the performance of ionic-polymer-metal composite sensors. Smart Mater Struct. 2010;19(7):075002.
45. He Q, Liu Z, Yin G, Yue Y, Yu M, Li H, et al. The highly stable air-operating ionic polymer metal composite actuator with consecutive channels and its potential application in soft gripper. Smart Mater Struct. 2020;29(4):045013.

Supplementary material

The following online material is available for this article:

Figure SI.1 - IPMC-Li and IPMC-K water uptake as a function of time for a) RH = 30%, b) RH = 60%, and c) RH = 60%. The osmotic equilibrium is achieved when sample mass varies by less than 5%.